Journal Pre-proof

CRISPR mediated base conversion allows discriminatory depletion of endogenous T cell receptors for enhanced synthetic immunity

Roland Preece, Andrea Pavesi, Soragia Athina Gkazi, Kerstin A. Stegmann, Christos Georgiadis, Zhi Ming Tan, Jia Ying Joey Aw, Mala K. Maini, Antonio Bertoletti, Waseem Qasim

Please cite this article as: Preece R, Pavesi A, Gkazi SA, Stegmann KA, Georgiadis C, Tan ZM, Joey Aw JY, Maini MK, Bertoletti A, Qasim W, CRISPR mediated base conversion allows discriminatory depletion of endogenous T cell receptors for enhanced synthetic immunity, *Molecular Therapy: Methods & Clinical Development* (2020), doi: https://doi.org/10.1016/j.omtm.2020.09.002.

This is a PDF file of an article that has undergone enhancements after acceptance, such as the addition of a cover page and metadata, and formatting for readability, but it is not yet the definitive version of record. This version will undergo additional copyediting, typesetting and review before it is published in its final form, but we are providing this version to give early visibility of the article. Please note that, during the production process, errors may be discovered which could affect the content, and all legal disclaimers that apply to the journal pertain.
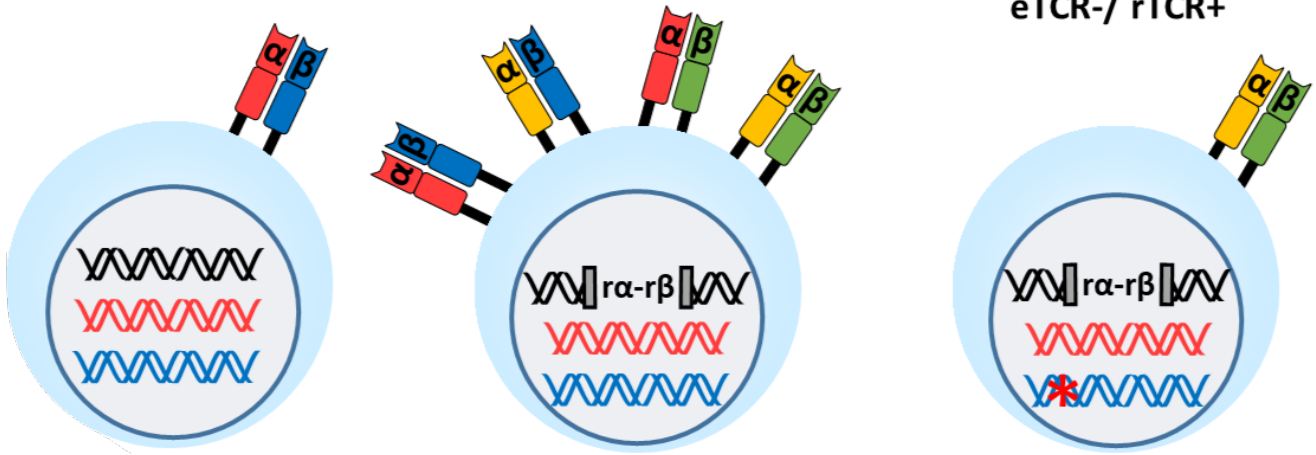
Unmodified T cells: **Lentiviral transduced:** **Lentiviral transduced + *TRBC***

eTCR-/ rTCR+

Genomic DNA:

***TRAC* locus:**

***TRBC1/2* locus:**

***TRBC1/2* locus knockout:**

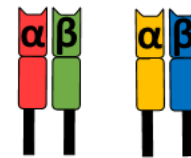**Lentiviral integration:** rα-rβ

Endogenous TCR:

Recombinant TCR:

Possible mispairing:

1 **CRISPR mediated base conversion allows discriminatory depletion of endogenous T cell**

2 **receptors for enhanced synthetic immunity.**

3

4 **Authors:** Roland Preece[1], Andrea Pavesi[2], Soragia Athina Gkazi[1], Kerstin A. Stegmann[3],

5 Christos Georgiadis[1], Zhi Ming Tan[2], Jia Ying Joey Aw[2], Mala K. Maini[3], Antonio Bertoletti[4, 5],

6 Waseem Qasim[1]

7

8 [1]Molecular and Cellular Immunology Unit, UCL Great Ormond Street Institute of Child

9 Health, London, WC1N 1EH. NIHR Great Ormond Street Hospital Biomedical Research

10 Centre, 30 Guilford Street, London.

11

12 [2]Institute of Molecular and Cell Biology (IMCB), Agency for Science, Technology and

13 Research (A*STAR) 61 Biopolis Drive, Singapore 138673

14

15 [3]UCL Division of Infection and Immunity, The Rayne Building, 5 University Street London,

16 WC1E 6EJ

17

18 [4]Program Emerging Infectious Diseases, Duke-NUS Medical School, Singapore.

19

20 [5]Singapore Immunology Network (SigN), Agency of Science technology and Research

21 (A*STAR), Singapore

22

23

24

25 **Abstract:**

26 Emerging base editing technology exploits CRISPR RNA-guided DNA modification effects for

27 highly specific C>T conversion which has been used to efficiently disrupt gene expression.

28 These tools can enhance synthetic T cell immunity by restricting specificity, addressing HLA

29 barriers and promoting persistence. We report lentiviral delivery of a Hepatitis B virus (HBV)

30 specific recombinant TCR (rTCR) and a linked CRISPR single-guide RNA for simultaneous

31 disruption of endogenous TCRs (eTCR) when combined with transient cytosine deamination.

32 Discriminatory depletion of eTCR and coupled expression of rTCR resulted in enrichment of

33 HBV specific populations from 55% (SEM ± 2.4%) to 95% (SEM ± 0.5%). Intensity of rTCR

34 expression increased 1.8-2.9 fold compared to cells retaining their competing eTCR and

35 increased cytokine production and killing of HBV antigen-expressing hepatoma cells in a 3D

36 microfluidic model was exhibited. Molecular signatures confirmed seamless conversion of

37 C>T (G>A) had created a premature stop codon in TCR beta constant 1/2 loci, with no

38 notable activity at predicted off-target sites. Thus, targeted disruption of eTCR by cytosine

39 deamination and discriminatory enrichment of antigen-specific T cells offers the prospect of

40 enhanced, more specific T cell therapies against HBV associated hepatocellular carcinoma

41 (HCC) as well as other viral and tumour antigens.

42

43

44

45

46

47

48

49 **Lay Summary:**

50 White blood cells called T cells mediate powerful antiviral effects that can be used to target

51 liver cancers linked to Hepatitis B virus infection. We report new techniques that change the

52 DNA code in T cells and reprogram them to only recognise cells that show a particular

53 Hepatitis-B flag on their surface. Ultimately such approaches could allow banks of healthy

54 donor T cells to be created and used in multiple patients against viruses and certain cancers.

55 **Introduction:**

56 T cells redirected with recombinant T cell receptors (rTCR) are being investigated in early

57 phase human studies [1-3]. Limitations include unpredictable 'off-target effects' due to TCR

58 cross-reactivity, for example cardiac toxicity following therapy with MAGE-A3 rTCR [4, 5] and

59 concerns that endogenous TCR α and β chains may miss-pair with rTCR chains and give rise

60 to novel dimeric complexes with unpredictable specificities [6, 7]. These limitations have been

61 partially mitigated by predictive modelling of rTCR cross-reactivity and by promoting

62 exclusive rTCR pairing via additional disulfide bonds and other strategies [8-11]. Also of note is

63 the importance of rTCR assembly on the cell surface as a multimeric complex with CD3

64 chains, as competition from the endogenous TCR (eTCR) for the shared components can

65 limit cell surface expression [12]. Competition for such cellular components can be addressed

66 either by overexpression of CD3, disruption of eTCR by RNA interference [13], or nuclease

67 mediated genetic disruption of eTCR chains. Previously, zinc finger nucleases (ZFNs) [14],

68 transcription activator-like effector nucleases (TALENs) [15], and clustered regularly

69 interspaced short palindromic repeats (CRISPR)/CRISPR-associated protein 9 (Cas9) have all

70 been used to disrupt one or both TCR α and β chains [16-18]. These genome editing approaches

71 also reduce the likelihood of mispairing, but existing nuclease-based approaches all result in

72 double stranded DNA breaks and may create large insertions/deletions (indels), trigger

73 translocation events, and increase activation of p53 pathways [19-23]. Recently, a report of

74 autologous anti-tumour therapy with T cells edited using Cas9 to disrupt both TCR and PD1

75 expression noted readily detectable chromosomal translocations in the infused products [24],

76 and similar aberrations were found after TALEN editing of T cells modified to express anti-

77 CD19 chimeric antigen receptors [25].

78

79　　Here we report the application of emerging cytosine deaminase base editing technology for

80　　efficient and seamless base conversion to introduce premature stop codons in homologous

81　　regions of T cell receptor beta constant 1 and 2 (*TRBC 1/2*) chains [26, 27]. BE3 is a CRISPR

82　　guided nickase Cas9 (D10A), fused to a rat apolipoprotein B mRNA editing enzyme catalytic

83　　polypeptide (rAPOBEC1) deaminase at the N-terminus, which operates within a 4-8bp

84　　window distal to the protospacer adjacent motif (PAM) sequence. The inclusion of a C-

85　　terminus fusion comprising a uracil-DNA glycosylase inhibitor (UGI) (derived from *Bacillus*

86　　*subtilis* bacteriophage PBS1) inhibits uracil-DNA glycosylase and blocks uracil excision

87　　promoting conversion to thymidine as cells replicate. High levels of C>T conversion and low

88　　levels of indels have been reported for this third generation base editor (BE3) [28-30]. Here we

89　　investigate a codon optimized BE3 (coBE3) in the context of engineering T cells against

90　　Hepatitis B virus surface antigen, an important target in the treatment of hepatocellular

91　　carcinoma (HCC) [31, 32]. HBV viral antigens are processed and presented by major

92　　histocompatibility complex (MHC) molecules on the surface of infected cells [33, 34], and

93　　naturally occurring HBV-specific T cells, can engage with peptides presented in the context

94　　of HLA, to moderate viral and tumour burdens [35, 36]. Nevertheless, such HBV specific T cell

95　　responses can become exhausted during chronic HBV infection [37-39] and synthetic HBV-

96　　specific T cells can be generated through the expression of rTCRs [40-44]. The approach has

97　　already been tested clinically in HBV associated HCC, [45, 46] with further studies planned.

98　　Lentiviral vector delivery of a rTCR specific for HLA-A2/HBV peptide S183-91, incorporating

99　　murine constant regions, and coupled to a CRISPR single guide RNA (sgRNA) targeting

100　　*TRBC1/2* loci resulted in high levels of targeted cytosine deamination after transient delivery

101　　of mRNA encoding coBE3. Thereafter, discriminatory removal of residual eTCR+ cells was

102　　achieved by magnetic bead-mediated depletion using the anti-human TCRαβ monoclonal

103 antibody. Consequently rTCR expression was enriched, as the murine constant regions lack

104 the specific epitope recognised by this antibody. Phenotypic and functional assessments,

105 including migration and killing in a 3D microfluidic model verified immunotherapeutic

106 effects following genome editing, and molecular analysis of both DNA and RNA was

107 performed to examine editor effects.

108

109 **Results:**

110 **Base conversion disrupts eTCR expression and allows enrichment of T cells expressing**

111 **rTCR**

112 A third generation self-inactivating (SIN) lentiviral vector was generated encoding an HLA-

113 A0201 restricted rTCR (S183-91, FLLTRILTI) specific for HBV envelope protein [56] and a linked

114 sgRNA expression cassette targeting *TRBC 1/2*. The latter was embedded within a deleted

115 unique (ΔU3) region of the 3' long terminal repeat (LTR) under the transcriptional control of

116 an RNA polymerase III human U6 promoter as previously described [47]. This configuration is

117 referred to as terminal-TRBC-S183-91 rTCR (TTRBC-S183-91 rTCR) (Figure 1). Upon

118 electroporation of coBE3 mRNA, the sgRNA mediated highly targeted base conversion of

119 two neighbouring cytosine nucleotides within exon 1 of *TRBC 1 /2* loci. Single or double base

120 conversion produces a premature stop codon within a 4-8bp window distal to the nCas9

121 (D10A) PAM sequence (Figure2A). Consequently, disruption of endogenous TCR β chain

122 expression eliminated eTCRαβ assembly, and the inclusion of murine constant regions

123 within the rTCR further addressed any possibility of aberrant cross-pairing between residual

124 recombinant and endogenous chains (Figure 2B). Following the timeline shown in Figure 2C,

125 healthy T cells were readily activated and transduced resulting in 50-60% rTCR expression

126 (Figure 2D and E i). Exposure to coBE3 led to disruption of eTCR expression and

127   simultaneous emergence of rTCR+ populations, increasing in proportion to approximately

128   60-65% of the cultures (Figure 2D and 2E i). Furthermore, because eTCR was amenable to

129   detection by anti-TCRαβ monoclonal antibody, magnetic bead-mediated depletion of

130   residual eTCRαβ expressing cells was possible. Notably, rTCR (constructed with murine C

131   domains) was not susceptible to these reagents and thus at the end of production, cells

132   could be enriched for endogenous TCR-/ recombinant TCR+ (eTCR-/rTCR+), resulting in a

133   highly homogenous product (>99% eTCR-/ 95.9% rTCR+) (Figure 2D and Ei). There was also a

134   significant increase in the mean florescence intensity (MFI) of rTCR in eTCR-/rTCR+ cells

135   compared to eTCR+/rTCR±, suggesting enhanced cell surface expression of rTCR in the

136   absence of eTCR, which may otherwise have competed for CD3 chains during assembly (one

137   way ANOVA, p<0.02) (Figure 2E ii).

138

Hepatitis B antigen specific responses of eTCR-/rTCR+ T cells

140   Three different *in vitro* assessments of antigen specific function were undertaken. Firstly,

141   production of cytokines including interferon-γ (IFNγ), tumor necrosis factor-α (TNFα),

142   interleukin-2 (IL-2), and C-C motif chemokine ligand 4 (CCL4) was determined by flow

143   cytometry in T cells responding to HepG2 cells pulsed with the irrelevant control peptide

144   (HBV core C18-27, FLPSDFFPSV) or a gradient of Hepatitis B target surface envelope peptide

145   (S183-91, FLLTRILTI) concentrations. In all three donors tested, cytokine production was

146   higher in eTCR-/rTCR+ T cells in response to target S183-91 peptide (Figure 3A i and ii), with

147   absent response to control C18-27 peptide and no-peptide control (Figure S1). Next, we

148   investigated effector function at different E:T ratios in a previously described XCelligence

149   impedance assay and calculated the relevant normalised cell indices over 72 hours after

150   addition of effector T cells [55]. An increased index indicated HepG2 target cell proliferation,

151 whereas cell death or apoptosis resulted in a reduced index, signifying higher levels of

152 effector T cell activity (Figure 3B). Control groups included target cells alone (HepG2 alone),

153 and non-transduced effectors (eTCR+/rTCR-), where as expected, there was a progressive

154 increase and plateau in index. In contrast, both effector groups exhibited a transient rise

155 and then decline in index, with more rapid reductions mediated by eTCR-/rTCR+ cells

156 compared to eTCR+/rTCR± T cells at all E:T ratios (Figure 3C i). Overall effector function was

157 calculated by area under the curve as shown in Figure 3C ii, reflecting the increased

158 cytotoxicity by enriched eTCR-/rTCR+ effector cells compared to their unedited, non eTCR

159 depleted counterparts (eTCR+/rTCR±).

160 Finally, migration and target cell killing by engineered T cells was determined in a 3D

161 microfluidics device. The system captured migration of effector T cells from a fluidics

162 channel to a collagen gel embedded with target PreS1-GFP-HepG2 cells. Phenotyping of

163 effector T cells confirmed rTCR expression (Figure 4A) and minimal cytokine expression in

164 the absence of stimulation after thawing. Comparable numbers of T cells were observed

165 migrating into the gel between the effector groups (Figure S2) before cytokine expression

166 profiles were compared between cells recovered from inside or outside the gel area (Figure

167 4B). Both eTCR+/rTCR± and eTCR-/rTCR+ effector groups presented higher levels of IL-2,

168 INFγ, and TNFα expression within the gel. Killing of PreS1-GFP-HepG2 cells by eTCR-/rTCR+

169 cells was confirmed within 24 hours whereas eTCR+/rTCR± cells at this time point were

170 comparable to control eTCR+/rTCR- indices and the control PreS1-GFP-HepG2 alone groups

171 (Figure 4C). Direct visualisation revealed greater clearance of HepG2 cells after co-culture

172 with eTCR-/rTCR+ T cells (Figure 4D).

173

174 **Molecular characterisation of base editor effects**

175   The application of novel genome editing tools necessitated further investigation of

176   anticipated and unexpected molecular consequences of T cell engineering. There is an

177   established experience of lentiviral mediated effects, including their propensity to integrate

178   into transcriptionally active genes [57-59] and we did not re-examine these aspects. However,

179   base conversion effects of coBE3 were characterised in depth, extending comparisons to the

180   effects of SpCas9 disruption in similar experiments disrupting eTCR expression in T cells

181   engineered to express a CAR against CD19. Both modalities had mediated high levels of

182   TCRαβ disruption (coBE3: 40.4% ± SEM 5.4%, SpCas9: 52.7% ± SEM 6%) (n=4, Figure S3) but

183   as anticipated we found reduced indel frequencies following electroporation of coBE3 (11.9%

184   ± SEM 1.8%) compared to SpCas9 delivery (48.7% ± SEM 6%).

185   In the context of rTCR delivery, direct sequencing of *TRBC 1/2* in TCRαβ depleted eTCR-

186   /rTCR+ T cells was undertaken and analysed using EditR, with cytosines at positions 5 and 6

187   distal to the PAM of particular interest (Figure 5A i and ii). High levels of C>T conversion

188   (G>A sense strand) were captured at these positions (37.3 ± SEM 3.9% and 24.3 ± SEM 2.2%

189   at C5 and C6 respectively), with little activity at other nearby C residues (5 ± SEM 1.2% C1,

190   2.3 ± SEM 1% C2, and 4.3 ± SEM 1.8% C3). NGS revealed similar levels of C>T conversion at

191   both positions C5 (40 ± SEM 2.9%) and C6 (32.3 ± SEM 3%) (Figure S4). Although mostly

192   seamless, a minority of reads exhibited small (<10bp, 8.4 ± SEM 1.4%) or large (10-100bp,

193   8.2 ± SEM 0.7%) indels signatures (Figure 5A iii) as others have noted previously [28-30].

194   *In silico* analysis of sgRNA binding and possible off-target activity was undertaken using

195   Benchling and presented no exonic off-targets with <3 mismatches. Six genomic loci with

196   the highest scores for off-target activity, all of which contained cytosine bases within the

197   BE3 editing window were interrogated directly by NGS in three different donors (Figure 5B).

198   We found very low levels (<1%) of conversion activity at these sites, and only one intronic

199 site exhibited C>T changes higher than in its respective non-edited control sample. Recent

200 reports in cell lines have also suggested that promiscuous rAPOBEC1 RNA deamination

201 (including by BE3) can arise following plasmid mediated expression of base editors [60-63]. In

202 the T cell context, and with coBE3 transiently expressed by mRNA electroporation we

203 investigated if regions directing antigen receptor specificity might be affected. Analysis of

204 RNA from T cells exposed to coBE3 focussed on high throughput interrogation of TCR

205 hypervariable regions (TCRVα and TCRVβ CDR3 regions). Analysis of samples collected at

206 serial time points, from 1-8 days post BE3 mRNA delivery, found no obvious evidence of

207 aberrant deamination compared to controls (99-100% cysteines unmodified) and intact

208 sequence integrity of HBs183-91 rTCR was verified (Figure 5C). In addition, transcriptomic

209 analysis on these samples detected anticipated effects of T cell activation and transduction

210 over time (Figure S5). Thus the first principal component (PC1), accounted for 76% of

211 variance when comparing day 5 and day 12. As the second principal component (PC2)

212 accounted for only 13% of variance, no major transcriptional changes between edited and

213 non-edited cells were noted. *In silico* analysis had identified a further 24 unique sites of

214 possible off-target BE activity in exonic regions. However, these were all found to have low

215 transcriptional activity (averaged < 100 reads) in both edited and non-edited T cells and

216 therefore unlikely to be of importance.

217 Thus, while on-target deamination and creation of TCR-stop codons was highly efficient,

218 there was no notable activity at sites of potential interest at either the DNA or RNA level for

219 coBE3.

220

221 **Discussion:**

222   T cell immunotherapy against conventional tumour-associated targets such as NY-ESO-1 are

223   being widely investigated, and recent reports indicate autologous T cells with additional

224   CRISPR/Cas9 modifications designed to improve persistence and efficacy can be safely

225   infused [24, 64]. Emerging base editor technologies offer the prospect of highly specific C>T

226   (G>A) base conversion that can be harnessed to create seamless premature stop codons or

227   modify splice sites to disrupt gene expression for advanced T cell engineering.

228   We previously reported the first therapeutic use of autologous T cells modified to express

229   HBsAg specific T cell receptors in a subject with chemoresistant, extrahepatic, metastatic

230   disease. In that case, HBV antigens were detectable in HCC metastases but not in donor-

231   derived liver (following cadaveric liver transplantation) thereby reducing the risk of T cell-

232   mediated hepatitis. Gene-modified T cells survived, expanded and mediated a reduction in

233   HBsAg levels and whilst efficacy was not established, there was no significant on- or off-

234   target toxicity [2]. A small number of additional subjects have been treated subsequently,

235   although the approach remains highly patient-tailored and extending to larger numbers of

236   patients is logistically challenging and costly. Similar hurdles are being addressed in the

237   arena of haematological malignancies through the generation of 'universal' T cells

238   expressing CARs from non-HLA matched healthy donors. As such, depletion of endogenous

239   TCR and other antigens by genome editing has allowed HLA barriers to be circumvented,

240   and ongoing trials suggest that such universal CAR T cells can expand and persist sufficiently

241   to induce molecular remission [25]. The editing tools applied in clinic have included TALENS

242   and CRISPR/Cas9, and rely on targeted DNA cleavage and repair by non-homologous end

243   joining (NHEJ) which results in the creation of indels leading to gene disruption. Application

244   of CRISPR guided base conversion to create stop codons or alter critical splice site to disrupt

245   gene expression offers the possibility of seamless gene disruption with greatly reduced

246   likelihood of translocations or toxicity. We report the application of APOBEC deaminase

247   technology for the generation of engineered T cells, which are then rendered devoid of

248   endogenous TCRs and uniformly express rTCR specific for an epitope of HBsAg. The resulting

249   product was homogenous and exhibited enhanced rTCR intensity, greater levels of cytokine

250   production and antigen specific functional integrity in models of HCC elimination. An ability

251   to discriminate and selectively process, and deplete eTCR T cells while rTCR populations are

252   untouched provides critical advantages, especially for strategies when allogeneic donor cells

253   bearing potentially alloreactive eTCRs can be eliminated. Non-human protein sequences

254   within constructs have the potential to be immunogenic, although murine TCR constant

255   regions are considered unlikely determinants in the generation of human anti-mouse

256   antibodies [65]. Likewise, the BE configurations employ bacterial and rodent derived elements,

257   but expression is transient during *ex vivo* culture and unlikely to be problematic *in vivo*.

258   The rapid development of tools enabling highly targeted base conversion through

259   deamination effects promises tantalising opportunities, although in depth characterisation

260   of desirable and unwanted effects in subsequent therapeutic applications have to be

261   mapped. Existing CRISPR/Cas base-editors employing rAPOBEC1 (including coBE3) are

262   known to mediate off-target DNA edits and transcriptome-wide RNA deamination in both

263   protein-coding and non-coding regions [60-62]. While these could be problematic, newer

264   variants with more precise DNA restricted editing are already in development and should

265   continue to evolve as ever more efficient, specific and non-toxic editing tools. Our analysis

266   of possible off-target sgRNA activity in three donors found minimal base conversion effects

267   at predicted DNA sites. Importantly, examination of RNA detected no major differences in

268   gene expression levels between base edited and non-edited T cells, with only very minor

269   perturbations and C>U conversions of the CDR3 variable regions, no greater than in control

270   cells. Such changes could otherwise redirect the specificity of the introduced TCR, and

271   would risk causing autoimmunity or off-target T cell effects.

272   **Conclusion:**

273   Removal of eTCR enhances expression of introduced rTCR, reduces the risk of aberrant

274   cross-pairing, and allows discriminatory enrichment of engineered T cells. The strategy also

275   opens the door to generating 'universal' allogeneic T cells from healthy HLA-mismatched

276   donors by reducing the risk of graft versus host disease. In the case of the rTCR specific for

277   HBs183-91, blood from healthy HLA-A201 donors could readily be further edited to disrupt

278   mismatched HLA molecules creating immunologically stealthy cells. Additional multiplexed

279   editing of T cell exhaustion markers may promote enhanced persistence and anti-tumour

280   effects. Ultimately, pre-manufactured banks of eTCR-/rTCR+ T cells specific for groups of

281   dominant HLA/peptide combinations could provide treatment options for large numbers

282   subjects.

283

284   **Materials and Methods:**

285   **CRISPR guide RNA**

286   Guide sequences compatible with coBE3 targeting homologous sequences in *TRBC1* and *2*

287   were designed using the CRISPR design tool, Benchling (https://benchling.com) and

288   provided an on-target editing score for predicted activity at each cytosine around the

289   editing window [28]. TRBC1/2: $C_{0.8}C_{11}C_{5.7}AC_{21.9}$ $C_{21.4}$AGCUCAGCUCCACG (anti-sense, numbers

290 indicate predicted editing scores for the specific cytosine base). Predicted exonic off-target

291 binding required at least 3 mismatches within the protospacer.

292

293 **Lentiviral construct for rTCR and sgRNA delivery**

294 Lentiviral design for coupled transgene and guide RNA expression has been previously

295 described [47]. Briefly, rTCR HLA-A0201/HBs183-91 was cloned under the control of an

296 internal human phosphoglycerate kinase 1 (hPGK) promoter and a CRISPR guide expression

297 cassette was embedded in the lentiviral 3' LTR. This comprised a 5' RNA polymerase III

298 promoter (U6) and a sgRNA specific for TCRB1/2 with a 5'G for improved transcription.

299 Vector stocks were produced in 293T cells by transient transfection with third generation

300 packaging plasmids and concentrated by ultracentrifugation prior to storage at -80°C.

301

302 **Primary human lymphocyte culture and modification**

303 Peripheral blood mononuclear cells (PBMCs) were isolated by ficoll density gradient and

304 subsequently activated with TransAct reagent (130-111-160, Miltenyi Biotec) at 10μl/ml.

305 TexMACS medium (130-097-196, Miltenyi Biotec) with 3% human AB serum (GEM-100-512-

306 HI, Seralabs) and 100U/ml IL-2 was used for all lymphocyte cell culture. Transduction with

307 lentiviral vector was performed 24 hours post activation at a multiplicity of infection (MOI)

308 of 5. Electroporation of coBE3 mRNA was performed at day 4 post activation, after which

309 cells were cultured in a G-Rex®10 (P/N 80040S, Wilsonwolf). Lymphocytes were cultured for

310 11 days post activation and magnetically depleted using anti-TCR α/β-biotin (130-098-219,

311 Miltenyi Biotec) followed by incubation with anti-biotin microbeads ultrapure (130-105-637,

312 Miltenyi Biotec) and separation through LD columns (130-042-901, Miltenyi Biotec). Cells

313 were rested overnight before flow cytometry based phenotyping and cryopreservation.

314

315 **Phenotyping Flow cytometry**

316 Flow cytometry was performed on a 4-laser BD LSRII (BD Biosciences), with subsequent

317 analysis executed using FlowJo v10 (TreeStar). Cells were stained according to

318 manufacturer's instructions with Mouse TCR β constant-APC (Clone H57-597, Biolegend, Cat

319 109211), Human TCRα/β-PerCP vio 700 (Clone REA652, Miltenyi Biotec, Cat 130-113-540),

320 PD1-PE (Clone PD1.3.1.3, Miltenyi Biotec, Cat 130-117-384), CD4-VioBlue (Clone REA623,

321 Miltenyi Biotec, Cat 130-114-534), and CD45-VioGreen (Clone REA747, Miltenyi Biotec, Cat

322 130-110-638).

323

324 **Antigen specific responses**

325 Target (T) HepG2 cells were pulsed with HBV surface envelope peptide S183-91 (FLLTRILTI,

326 JPT Peptide Technologies) and irrelevant control HBV core peptide C18-27 (FLPSDFFPSV, JPT

327 Peptide Technologies) peptide at gradient concentrations for 1h at 37°C. Cryopreserved

328 effector (E) T cells (eTCR+/rTCR-, eTCR+/rTCR±, and eTCR-/rTCR+) were thawed and cultured

329 at E:T ratio of 1:1 and 0.1μg/ml Brefeldin A (Sigma) was added before overnight co-culture.

330 A Fortessa X20 flow cytometer (BD) was used for cell acquisition, with FlowJo v10 (TreeStar)

331 used to analyse phenotype and function of effector T cells groups. Phenotyping included

332 intracellular staining with TNFα FITC (clone MAb11, BD biosciences, Cat 502906), MIP-1b PE

333 (clone D21-1351, BD biosciences, Cat 550078), IL-2 PerCP-eFlour710 (clone MQ1-17H12,

334 eBioscience, Cat 46-7029-42), GranzymeB AF700 (clone GB11, BD biosciences, Cat 560213),

335 IFNg V450 (clone B27, BD biosciences, Cat 560371), and surface staining with CD3 BUV395

336 (clone UCHT1, BD biosciences, Cat 563546) and mouse TCR β constant-APC (Clone H57-597,

337 Biolegend, Cat 109211).

338

Electroporation of base editor mRNA

340 The BE3 amino acid sequence was sourced from previously published work containing a

341 single C terminus nuclear localisation signal[28]. Additionally, the DNA sequence has been

342 codon optimised by ThermoFisher Scientific, GeneArt. coBE3 mRNA was produced by Trilink,

343 and clean-capped (Cap 1), polyadenylated and purified by high performance liquid

344 chromatography (HPLC). Electroporation used a 100µl tip-kit and Neon transfection system

345 (ThermoFisher Scientific). Cells were electroporated at 20×10^6 cells/ml in buffer T, using

346 protocol 24 (1600V, 10ms, 3pulses) with 50µg/ml coBE3 mRNA.

347 Following electroporation T cells were incubated overnight at 30°C before restoration to

348 37°C.

349

Molecular characterisation of on-target DNA editing

351 Genomic DNA extraction was performed using DNeasy Blood and Tissue Kit (69504, QIAGEN)

352 and PCR sequencing undertaken using primers for *TRBC1/2* loci. *TRBC* forward: 5'

353 AGGTCGCTGTGTTTGAGC 3', *TRBC* reverse: 5' CTATCCTGGGTCCACTCGTC 3'. Sanger

354 sequencing data (Eurofins Genomics) was analysed using EditR

355 (https://moriaritylab.shinyapps.io/editr_v10/) [48]. In addition amplified products were library

356 prepped for next generation sequencing (NGS) using a Nextera XT kit (Illumina, Cambridge,

357 UK). After the library preparation, individually barcoded samples were pooled and ran in a

358 MiSeq using a 500-V2 nano-cartridge. Demultiplexed fastq files were uploaded to Galaxy [49]

359 for trimming and alignment. NHEJ signatures were analysed using Pindel [50], haplotypes were

360 analysed using Freebayes [51]. Figures were created in R.

361

362 **Molecular characterisation of off-target DNA editing**

363 Online software, Benchling, was used to predict off-targets for the *TRBC* guide. Libraries

364 were prepared on the top six off-targets using the same methodology as above (NGS for on-

365 target DNA editing) and combinations of target-specific primers (Supplementary

366 Bioinformatics Methods).

367

368 **Characterisation and analysis of the transcriptome**

369 Sequential RNA samples from engineered T cells were prepared for RNA sequencing using

370 the KAPA mRNA Hyper prep kit (Roche) at UCL Genomics. Initial analysis was performed on

371 a customised Galaxy workflow followed by transcriptomics analysis on iDEP 9.1 (Workflow

372 using R packages). Online software tool, CRISPR RGEN 'Cas-OFFinder', predicted 1,071 off-

373 target sites for TRBC guide with parameters set for up to 3 mismatches and a 1 nucleotide

374 bulge). A pipeline was developed for further investigation of these sites in RNAseq data

375 (Supplementary Bioinformatics Methods).

376

377 **Screening for rTCR RNA editing effects**

378 Total RNA was extracted using a QIAamp RNA Blood Mini kit (Qiagen, 52304) for TCR library

379 preparation and sequencing as previously described [52, 53]. rTCR RNA was reverse transcribed

380 using a murine TRBC specific primer (5' TGGACTTCTTTGCCGTTGAC 3'). Following ligation of

381 an oligonucleotide containing the Illumina SP2 primer and unique molecular identifiers,

382 products were amplified using primers specific to the murine constant alpha and beta

383 chains (5' CGTTGATCTGGCTGTCGAAG 3' and 5' TTGACCCACCAAGACAGCTC 3', respectively).

384 Finally, libraries were built in two furthers steps of amplification during which the SP1

385 sequencing primer, indices and Illumina adaptors were added. Part of the primers used in

386 these were also specific for the constant regions (5'

387 ACACTCTTTCCCTACACGACGCTCTTCCGATCTNNNNNNGCCAATGCACGTTGATCTGGCTGTCGAA

388 G   3'   and   5'

389 ACACTCTTTCCCTACACGACGCTCTTCCGATCTNNNNNNGCCAATCCGTTGACCCACCAAGACAGCT

390 C 3'). The final purified libraries were verified using Tapestation (Agilent) and Qubit (Thermo

391 Fisher Scientific), multiplexed and sequenced on a MiSeq system (Illumina) using 500-V2

392 cartridges (Illumina). Fastq files were demultiplexed using Demultiplexor

393 (https://github.com/innate2adaptive/Decombinator) [54]. Using Galaxy tools [49], the

394 demultiplexed fastq files were trimmed (Trim Galore and Trimmomatic) and aligned

395 (Bowtie2) to the relative TCR HBV gene map. Aligned files were interrogated for the

396 frequency of the reference sequence per base around the complementarity-determining

397 region 3 (CDR3) (100bp total window).

398

399 **Data availability**

400 All fastq files will be available on NCBI Sequence Read Archive upon publication (BioProject

401 ID: PRJNA637371).

402

403 **Xcelligence impedance assay**

404 Target HepG2 cells were seeded (1×10^5 per well) in the dedicated device (E-Plate VIEW 16,

405 ACEA Biosciences Inc.) and cultured for 24 hours. Impedance measurement was acquired

406 with an interval of 15 minutes by an array of electrodes located at the bottom of the plate.

407 Different T cell preparations and E:T ratios were added in the well after 24 hours, and the

408 impedance signal was recorded for the subsequent 72 hours. Three different donors were

409 tested in triplicate conditions.

410

411 **3D microfluidics device**

412 Briefly, dissociated PreS1-GFP-HepG2 target cells were mixed with collagen type I gel (rat

413 tail, Corning) and injected into the dedicated region of the 3D cell culture chip (DAX-1, AIM

414 Biotech), before gel polymerization, following a previously developed protocol [38, 43, 55]. R10

415 media with 3µM of DRAQ7 (Biolegend) cell-impermeable nuclear dye was then added to the

416 media channels to hydrate the gel, and chips were incubated at 37°C. T cells were stained

417 with 3µM Cell-Tracker Violet BMQC (Thermo Fisher Scientific) and were injected into one of

418 two media channels flanking the gel region before overnight incubation. 3D confocal images

419 were acquired daily with a high content imaging system (Phenix, Perkin Elmer). T cells from

420 the liquid channel were collected by manual pipetting; after, collagenase solution was

421 injected into the device to retrieve the immune cells migrating in the hydrogel region for

422 flow cytometer analysis on a 4-laser BD LSRII (BD Biosciences).

423

424 **Statistics**

425 Statistical analysis was performed using GraphPad Prism software, version 8.0.0.

426

433

Disclosures:

WQ holds interests unrelated to this project in Autolus Ltd.

WQ received unrelated research funding from Cellectis, Servier, Miltenyi, Bellicum.

References:

1. Morgan, RA, Dudley, ME, Wunderlich, JR, Hughes, MS, Yang, JC, Sherry, RM*, et al.* (2006). Cancer regression in patients after transfer of genetically engineered lymphocytes. *Science* **314**: 126-129.

2. Qasim, W, Brunetto, M, Gehring, AJ, Xue, SA, Schurich, A, Khakpoor, A*, et al.* (2015). Immunotherapy of HCC metastases with autologous T cell receptor redirected T cells, targeting HBsAg in a liver transplant patient. *J Hepatol* **62**: 486-491.

3. Chapuis, AG, Egan, DN, Bar, M, Schmitt, TM, McAfee, MS, Paulson, KG*, et al.* (2019). T cell receptor gene therapy targeting WT1 prevents acute myeloid leukemia relapse post-transplant. *Nature medicine* **25**: 1064-1072.

4. Linette, GP, Stadtmauer, EA, Maus, MV, Rapoport, AP, Levine, BL, Emery, L*, et al.* (2013). Cardiovascular toxicity and titin cross-reactivity of affinity-enhanced T cells in myeloma and melanoma. *Blood* **122**: 863-871.

5. Cameron, BJ, Gerry, AB, Dukes, J, Harper, JV, Kannan, V, Bianchi, FC*, et al.* (2013). Identification of a Titin-derived HLA-A1-presented peptide as a cross-reactive target for engineered MAGE A3-directed T cells. *Science translational medicine* **5**: 197ra103.

6. Bendle, GM, Linnemann, C, Hooijkaas, AI, Bies, L, de Witte, MA, Jorritsma, A*, et al.* (2010). Lethal graft-versus-host disease in mouse models of T cell receptor gene therapy. *NatMed* **16**: 565-570, 561p.

458   7.   van Loenen, MM, de Boer, R, Amir, AL, Hagedoorn, RS, Volbeda, GL, Willemze, R, *et*

459   *al.* (2010). Mixed T cell receptor dimers harbor potentially harmful neoreactivity.

460   *Proceedings of the National Academy of Sciences of the United States of America*

461   **107**: 10972-10977.

462   8.   Cohen, CJ, Zhao, Y, Zheng, Z, Rosenberg, SA, and Morgan, RA (2006). Enhanced

463   Antitumor Activity of Murine-Human Hybrid T-Cell Receptor (TCR) in Human

464   Lymphocytes Is Associated with Improved Pairing and TCR/CD3 Stability. *Cancer Res*

465   **66**: 8878-8886.

466   9.   Li, Y, Moysey, R, Molloy, PE, Vuidepot, AL, Mahon, T, Baston, E*, et al.* (2005).

467   Directed evolution of human T-cell receptors with picomolar affinities by phage

468   display. *Nature biotechnology* **23**: 349-354.

469   10.   Kuball, J, Dossett, ML, Wolfl, M, Ho, WY, Voss, RH, Fowler, C*, et al.* (2007).

470   Facilitating matched pairing and expression of TCR chains introduced into human T

471   cells. *Blood* **109**: 2331-2338.

472   11.   Bentzen, AK, Such, L, Jensen, KK, Marquard, AM, Jessen, LE, Miller, NJ*, et al.* (2018). T

473   cell receptor fingerprinting enables in-depth characterization of the interactions

474   governing recognition of peptide-MHC complexes. *Nature biotechnology*.

475   12.   Ahmadi, M, King, JW, Xue, SA, Voisine, C, Holler, A, Wright, GP*, et al.* (2011). CD3

476   limits the efficacy of TCR gene therapy in vivo. *Blood* **118**: 3528-3537.

477   13.   Bunse, M, Bendle, GM, Linnemann, C, Bies, L, Schulz, S, Schumacher, TN*, et al.*

478   (2014). RNAi-mediated TCR knockdown prevents autoimmunity in mice caused by

479   mixed TCR dimers following TCR gene transfer. *Molecular therapy : the journal of the*

480   *American Society of Gene Therapy* **22**: 1983-1991.

481   14.   Provasi, E, Genovese, P, Lombardo, A, Magnani, Z, Liu, PQ, Reik, A*, et al.* (2012).

482   Editing T cell specificity towards leukemia by zinc finger nucleases and lentiviral gene

483   transfer. *NatMed* **18**: 807-815.

484   15.   Berdien, B, Mock, U, Atanackovic, D, and Fehse, B (2014). TALEN-mediated editing of

485   endogenous T-cell receptors facilitates efficient reprogramming of T lymphocytes by

486   lentiviral gene transfer. *Gene therapy* **21**: 539-548.

487   16.   Legut, M, Dolton, G, Mian, AA, Ottmann, OG, and Sewell, AK (2018). CRISPR-

488   mediated TCR replacement generates superior anticancer transgenic T cells. *Blood*

489   **131**: 311-322.

490   17.   Roth, TL, Puig-Saus, C, Yu, R, Shifrut, E, Carnevale, J, Li, PJ*, et al.* (2018).

491   Reprogramming human T cell function and specificity with non-viral genome

492   targeting. *Nature* **559**: 405-409.

493   18.   Schober, K, Muller, TR, Gokmen, F, Grassmann, S, Effenberger, M, Poltorak, M*, et al.*

494   (2019). Orthotopic replacement of T-cell receptor alpha- and beta-chains with

495   preservation of near-physiological T-cell function. *Nat Biomed Eng* **3**: 974-984.

496   19.   Poirot, L, Philip, B, Schiffer-Mannioui, C, Le Clerre, D, Chion-Sotinel, I, Derniame, S*, et*

497   *al.* (2015). Multiplex Genome-Edited T-cell Manufacturing Platform for "Off-the-

498   Shelf" Adoptive T-cell Immunotherapies. *Cancer Res* **75**: 3853-3864.

499   20.   Adikusuma, F, Piltz, S, Corbett, MA, Turvey, M, McColl, SR, Helbig, KJ*, et al.* (2018).

500   Large deletions induced by Cas9 cleavage. *Nature* **560**: E8-E9.

501   21.   Haapaniemi, E, Botla, S, Persson, J, Schmierer, B, and Taipale, J (2018). CRISPR-Cas9

502   genome editing induces a p53-mediated DNA damage response. *Nature medicine*.

503   22.   Ihry, RJ, Worringer, KA, Salick, MR, Frias, E, Ho, D, Theriault, K*, et al.* (2018). p53

504   inhibits CRISPR-Cas9 engineering in human pluripotent stem cells. *Nature medicine*

505   **24**: 939-946.

506   23.   Kosicki, M, Tomberg, K, and Bradley, A (2018). Repair of double-strand breaks

507   induced by CRISPR-Cas9 leads to large deletions and complex rearrangements.

508   *Nature biotechnology* **36**: 765-771.

509   24.   Stadtmauer, EA, Fraietta, JA, Davis, MM, Cohen, AD, Weber, KL, Lancaster, E*, et al.*

510   (2020). CRISPR-engineered T cells in patients with refractory cancer. *Science* **367**.

511   25.   Qasim, W, Zhan, H, Samarasinghe, S, Adams, S, Amrolia, P, Stafford, S*, et al.* (2017).

512   Molecular remission of infant B-ALL after infusion of universal TALEN gene-edited

513   CAR T cells. *Science translational medicine* **9**.

514   26.   Billon, P, Bryant, EE, Joseph, SA, Nambiar, TS, Hayward, SB, Rothstein, R*, et al.*

515   (2017). CRISPR-Mediated Base Editing Enables Efficient Disruption of Eukaryotic

516   Genes through Induction of STOP Codons. *Mol Cell* **67**: 1068-1079 e1064.

517   27.   Kuscu, C, Parlak, M, Tufan, T, Yang, J, Szlachta, K, Wei, X*, et al.* (2017). CRISPR-STOP:

518   gene silencing through base-editing-induced nonsense mutations. *Nature methods*

519   **14**: 710-712.

520   28.   Komor, AC, Kim, YB, Packer, MS, Zuris, JA, and Liu, DR (2016). Programmable editing

521   of a target base in genomic DNA without double-stranded DNA cleavage. *Nature*

522   **533**: 420-424.

523   29.   Komor, AC, Zhao, KT, Packer, MS, Gaudelli, NM, Waterbury, AL, Koblan, LW*, et al.*

524   (2017). Improved base excision repair inhibition and bacteriophage Mu Gam protein

525   yields C:G-to-T:A base editors with higher efficiency and product purity. *Sci Adv* **3**:

526   eaao4774.

527   30.   Webber, BR, Lonetree, CL, Kluesner, MG, Johnson, MJ, Pomeroy, EJ, Diers, MD*, et al.*

528   (2019). Highly efficient multiplex human T cell engineering without double-strand

529   breaks using Cas9 base editors. *Nature communications* **10**: 5222.

530   31.   Sung, WK, Zheng, H, Li, S, Chen, R, Liu, X, Li, Y*, et al.* (2012). Genome-wide survey of

531   recurrent HBV integration in hepatocellular carcinoma. *Nature genetics* **44**: 765-769.

532   32.   Amaddeo, G, Cao, Q, Ladeiro, Y, Imbeaud, S, Nault, JC, Jaoui, D*, et al.* (2015).

533   Integration of tumour and viral genomic characterizations in HBV-related

534   hepatocellular carcinomas. *Gut* **64**: 820-829.

535   33.   Brechot, C, Pourcel, C, Louise, A, Rain, B, and Tiollais, P (1980). Presence of

536   integrated hepatitis B virus DNA sequences in cellular DNA of human hepatocellular

537   carcinoma. *Nature* **286**: 533-535.

538   34.   Edman, JC, Gray, P, Valenzuela, P, Rall, LB, and Rutter, WJ (1980). Integration of

539   hepatitis B virus sequences and their expression in a human hepatoma cell. *Nature*

540   **286**: 535-538.

541   35.   El-Serag, HB (2011). Hepatocellular carcinoma. *N Engl J Med* **365**: 1118-1127.

542   36.   Chen, XP, Long, X, Jia, WL, Wu, HJ, Zhao, J, Liang, HF*, et al.* (2019). Viral integration

543   drives multifocal HCC during the occult HBV infection. *J Exp Clin Cancer Res* **38**: 261.

544   37.   Ye, B, Liu, X, Li, X, Kong, H, Tian, L, and Chen, Y (2015). T-cell exhaustion in chronic

545   hepatitis B infection: current knowledge and clinical significance. *Cell Death Dis* **6**:

546   e1694.

547   38.   Otano, I, Escors, D, Schurich, A, Singh, H, Robertson, F, Davidson, BR*, et al.* (2018).

548   Molecular Recalibration of PD-1+ Antigen-Specific T Cells from Blood and Liver.

549   *Molecular therapy : the journal of the American Society of Gene Therapy* **26**: 2553-

550   2566.

551   39.   Schuch, A, Salimi Alizei, E, Heim, K, Wieland, D, Kiraithe, MM, Kemming, J*, et al.*

552   (2019). Phenotypic and functional differences of HBV core-specific versus HBV

553   polymerase-specific CD8+ T cells in chronically HBV-infected patients with low viral

554   load. *Gut* **68**: 905-915.

555   40.   Sastry, KS, Too, CT, Kaur, K, Gehring, AJ, Low, L, Javiad, A*, et al.* (2011). Targeting

556   hepatitis B virus-infected cells with a T-cell receptor-like antibody. *Journal of virology*

557   **85**: 1935-1942.

558   41.   Koh, S, Shimasaki, N, Suwanarusk, R, Ho, ZZ, Chia, A, Banu, N*, et al.* (2013). A

559   practical approach to immunotherapy of hepatocellular carcinoma using T cells

560   redirected against hepatitis B virus. *Molecular therapy Nucleic acids* **2**: e114.

561   42.   Bertoletti, A, Brunetto, M, Maini, MK, Bonino, F, Qasim, W, and Stauss, H (2015). T

562   cell receptor-therapy in HBV-related hepatocellularcarcinoma. *Oncoimmunology* **4**:

563   e1008354.

564   43.   Pavesi, A, Tan, AT, Koh, S, Chia, A, Colombo, M, Antonecchia, E*, et al.* (2017). A 3D

565   microfluidic model for preclinical evaluation of TCR-engineered T cells against solid

566   tumors. *JCI Insight* **2**.

567   44.   Kah, J, Koh, S, Volz, T, Ceccarello, E, Allweiss, L, Lutgehetmann, M*, et al.* (2017).

568   Lymphocytes transiently expressing virus-specific T cell receptors reduce hepatitis B

569   virus infection. *The Journal of clinical investigation* **127**: 3177-3188.

570   45.   Qasim W, Amrolia PJ, Samarasinghe S, Ghorashian S, Zhan H, Stafford S*, et al.* (2015).

571   First Clinical Application of Talen Engineered Universal CAR19 T Cells in B-ALL. *Blood*

572   **126**: 2046.

573   46.   Tan, AT, Yang, N, Lee Krishnamoorthy, T, Oei, V, Chua, A, Zhao, X*, et al.* (2019). Use

574   of Expression Profiles of HBV-DNA Integrated Into Genomes of Hepatocellular

575   Carcinoma Cells to Select T Cells for Immunotherapy. *Gastroenterology* **156**: 1862-

576   1876 e1869.

577   47.   Georgiadis, C, Preece, R, Nickolay, L, Etuk, A, Petrova, A, Ladon, D*, et al.* (2018). Long

578   Terminal Repeat CRISPR-CAR-Coupled "Universal" T Cells Mediate Potent Anti-

579   leukemic Effects. *Molecular therapy : the journal of the American Society of Gene*

580   *Therapy*.

581   48.   Kluesner, MG, Nedveck, DA, Lahr, WS, Garbe, JR, Abrahante, JE, Webber, BR*, et al.*

582   (2018). EditR: A Method to Quantify Base Editing from Sanger Sequencing. *CRISPR J*

583   **1**: 239-250.

584   49.   Afgan, E, Baker, D, Batut, B, van den Beek, M, Bouvier, D, Cech, M*, et al.* (2018). The

585   Galaxy platform for accessible, reproducible and collaborative biomedical analyses:

586   2018 update. *Nucleic Acids Res* **46**: W537-W544.

587   50.   Ye, K, Schulz, MH, Long, Q, Apweiler, R, and Ning, Z (2009). Pindel: a pattern growth

588   approach to detect break points of large deletions and medium sized insertions from

589   paired-end short reads. *Bioinformatics* **25**: 2865-2871.

590   51.   Garrison, E, Marth, G (2012). Haplotype-based variant detection from short-read

591   sequencing.

592   52.   Oakes, T, Heather, JM, Best, K, Byng-Maddick, R, Husovsky, C, Ismail, M*, et al.* (2017).

593   Quantitative Characterization of the T Cell Receptor Repertoire of Naive and

594   Memory Subsets Using an Integrated Experimental and Computational Pipeline

595   Which Is Robust, Economical, and Versatile. *Front Immunol* **8**: 1267.

596   53.   Gkazi, AS, Margetts, BK, Attenborough, T, Mhaldien, L, Standing, JF, Oakes, T*, et al.*

597   (2018). Clinical T Cell Receptor Repertoire Deep Sequencing and Analysis: An

598   Application to Monitor Immune Reconstitution Following Cord Blood

599   Transplantation. *Front Immunol* **9**: 2547.

600 54. Thomas, N, Heather, J, Ndifon, W, Shawe-Taylor, J, and Chain, B (2013).

601   Decombinator: a tool for fast, efficient gene assignment in T-cell receptor sequences

602   using a finite state machine. *Bioinformatics* **29**: 542-550.

603 55. Lee, H, and Kim, JS (2018). Unexpected CRISPR on-target effects. *Nature*

604   *biotechnology* **36**: 703-704.

605 56. Gehring, AJ, Xue, SA, Ho, ZZ, Teoh, D, Ruedl, C, Chia, A*, et al.* (2011). Engineering

606   virus-specific T cells that target HBV infected hepatocytes and hepatocellular

607   carcinoma cell lines. *J Hepatol* **55**: 103-110.

608 57. Bushman, F, Lewinski, M, Ciuffi, A, Barr, S, Leipzig, J, Hannenhalli, S*, et al.* (2005).

609   Genome-wide Analysis of Retroviral DNA Integration. *Nature Reviews Microbiology*

610   **3**: 848-858.

611 58. Wang, GP, Ciuffi, A, Leipzig, J, Berry, CC, and Bushman, FD (2007). HIV integration

612   site selection: analysis by massively parallel pyrosequencing reveals association with

613   epigenetic modifications. *Genome Research* **17**: 1186-1194.

614 59. Cattoglio, C, Maruggi, G, Bartholomae, C, Malani, N, Pellin, D, Cocchiarella, F*, et al.*

615   (2010). High-definition mapping of retroviral integration sites defines the fate of

616   allogeneic T cells after donor lymphocyte infusion. *PLoSOne* **5**: e15688.

617 60. Grunewald, J, Zhou, R, Garcia, SP, Iyer, S, Lareau, CA, Aryee, MJ*, et al.* (2019).

618   Transcriptome-wide off-target RNA editing induced by CRISPR-guided DNA base

619   editors. *Nature* **569**: 433-437.

620   61.   Grunewald, J, Zhou, R, Iyer, S, Lareau, CA, Garcia, SP, Aryee, MJ*, et al.* (2019). CRISPR

621   DNA base editors with reduced RNA off-target and self-editing activities. *Nature*

622   *biotechnology* **37**: 1041-1048.

623   62.   Zhou, C, Sun, Y, Yan, R, Liu, Y, Zuo, E, Gu, C*, et al.* (2019). Off-target RNA mutation

624   induced by DNA base editing and its elimination by mutagenesis. *Nature* **571**: 275-

625   278.

626   63.   Gaudelli, NM, Lam, DK, Rees, HA, Sola-Esteves, NM, Barrera, LA, Born, DA*, et al.*

627   (2020). Directed evolution of adenine base editors with increased activity and

628   therapeutic application. *Nat Biotechnol* **38**: 892-900.

629   64.   Lu, Y, Xue, J, Deng, T, Zhou, X, Yu, K, Deng, L*, et al.* (2020). Safety and feasibility of

630   CRISPR-edited T cells in patients with refractory non-small-cell lung cancer. *Nature*

631   *medicine*.

632   65.   Davis, JL, Theoret, MR, Zheng, Z, Lamers, CH, Rosenberg, SA, and Morgan, RA (2010).

633   Development of human anti-murine T-cell receptor antibodies in both responding

634   and nonresponding patients enrolled in TCR gene therapy trials. *ClinCancer Res* **16**:

635   5852-5861.

636   66.   Gowthaman, R, and Pierce, BG (2018). TCRmodel: high resolution modeling of T cell

637   receptors from sequence. *Nucleic Acids Res* **46**: W396-W401.

638

639   **Figure 1: Terminal-CRISPR lentiviral vector configuration coupling HBV rTCR, and CRISPR**

640   **TRBC1/2 sgRNA delivery.** Lentiviral plasmid configuration, coupling the expression of a

641   recombinant T cell receptor (rTCR) against the hepatitis B virus (HBV) envelope surface

642   antigen 183-91 (S183-91) and a T cell receptor beta constant (TRBC)-specific single guide

643   RNA (sgRNA). The S183-91 rTCR is placed under the transcriptional control of an internal

644 human phosphoglycerate kinase 1 (hPGK) promoter, while TRBC1/2 sgRNA is expressed via

645 a human U6 promoter. The rTCR is expressed as a single transcript with the rTCR α chain

646 first, followed by the rTCR β chain separated by a porcine teschovirus-1 2A (P2A) self-

647 cleavage sequence. These recombinant chains are composed of the T cell receptor α

648 variable 34 (TRAV34), and the T cell receptor β variable 28 (TRBV28) domains, as well as

649 either murine TRAC (muTRAC), or murine TRBC 1 (muTRBC1). The rTCR chains contained an

650 additional cysteine-cysteine disulfide bond between murine constant regions. CMV:

651 Cytomegalovirus, cPPT: central polypurine tract, WPRE: woodchuck post-transcriptional

652 regulatory element, LTR: long terminal repeat, ΔU3: deleted unique 3', R: repeat, U5: unique

653 5', ψ: Psi, D: diversity region, J: joining region.

654

655 **Figure 2: Generation of eTCR-/rTCR+ T cells using coupled cytosine deaminase base editing.**

656 **A)** Schematic representation of base editor 3 (BE3) targeting exon 1 of the *TRBC 1/2* loci.

657 Editing window (blue) of the BE3 ranged from 4-8bp distal to PAM (red) with conversion of

658 Tryptophan (Trp) codons to create premature stop codons. **B)** Theoretical TCR chain pairing

659 when introducing a rTCR with or without knockout of the endogenous TCR β chain.

660 Incorporation of murine constant regions with an additional disulfide bridge in the

661 recombinant α and β (rα-rβ) chains reduced the potential for mispairing shown in the

662 middle panel and disruption of eTCR further reduces likelihood of mispairing. **C)** Schema of

663 cell production. Human peripheral blood lymphocytes were isolated and activated with

664 TransAct™ (anti-CD3/CD28) (day 0) before transduction (day 1) and electroporation with

665 codon optimised (co) BE3 mRNA (day 4). After overnight hypothermic culture at 30°C, cells

666 were expanded in G-Rex®10 flasks for seven days. Discriminatory depletion of residual

667 endogenous TCR (eTCR)-expressing cells was carried out (day 11), before cryopreservation

668 on day 14. **D)** Representative flow cytometry phenotyping of unmodified and Terminal-

669 TRBC-S183-91 rTCR (TTRBC-S183-91 rTCR) transduced cells. Delivery of coBE3 mRNA by

670 electroporation caused reduction of eTCR expression (38.1%) and emergence of eTCR-/

671 rTCR+ cells (Red box). Magnetic bead mediated depletion of residual eTCR+ T cells enriched

672 eTCR- populations, resulting in >99% eTCR-/ 95.9% rTCR+ (gated on CD45+). **E)** Expression of

673 S183-91 rTCR in three healthy donors. **i)** Histogram of rTCR (183-91) expression exhibiting

674 transduction ranging from 59.8%-63.9% in cells exposed to both vector and BE3, which

675 following TCRαβ bead-mediated depletion resulted in enrichment of genome edited cells,

676 with rTCR levels increased to 93.9%-96.1%. Three colours represent different donors. **ii)**

677 Levels of cell surface rTCR expression measured by mean fluorescence intensity (MFI) (n=3)

678 showed increased eTCR-/rTCR+ compared to eTCR+/rTCR± cells (gated on CD45+>rTCR+

679 population). One way ANOVA with Tukey's multiple comparison test, *p < 0.02*), error bars ±

680 1 standard error of the mean (SEM). nCas9: nickase CRISPR associated protein 9, UGI: uracil

681 DNA glycosylase inhibitor, rAPOBEC1: rat apolipoprotein B mRNA editing enzyme catalytic

682 polypeptide 1.

683

684 **Figure 3: Anti-HBV responsiveness of eTCR+/rTCR±, compared to base edited eTCR-/rTCR+**

685 **effector T cells. A)** Cytokine responses of effector T cells to HepG2 cell line pulsed with

686 target HBV surface peptide (S183-91, FLLTRILTI) n=3. **i)** Histograms of tumour necrosis factor

687 α (TNFα) responses to HepG2 target cells pulsed with 1µM target peptide. Both

688 eTCR+/rTCR± and eTCR-/rTCR+ effector groups are gated on CD45+>CD3+>rTCR+>CD8+,

689 whereas unmodifed eTCR+/rTCR- effectors are gated on CD45+>CD3+>rTCR->CD8+. Three

690 different colours represent results from three donors. **ii)** Cytokine responsiveness at

691 different concentrations of target peptide (S183-91). HepG2 target cells were pulsed with

692 1µM of control peptide (C18-27) to ensure specificity of response, showing comparable

693 cytokine responsiveness to the no peptide control. Effector groups eTCR+/rTCR± and eTCR-

694 /rTCR+ are gated on CD45+>CD3+>rTCR+>CD8+; whereas unmodified cells are gated on

695 CD45+>CD3+>rTCR->CD8+. Error bars ± 1 SEM. **B)** Schematic depiction of XCelligence

696 impedance assay showing cancer cells (green) seeded in wells with micro electrode array

697 (yellow), in the presence of effector T cells (blue). Where T cells recognise cancer cells, this

698 leads to cell death (brown) and reduced impedance resulting in lower cell index values, and

699 area under the curve (AUC). **C)** XCelligence data across different effector: target (E:T) ratios

700 (1:1, 1:2, and 1:4). **(i)** Visualisation of normalised cell index (NCI) over time, all donors

701 showed increased NCI with decreased E:T ratio. Both HepG2 alone (red), and eTCR+/rTCR-

702 (orange) show steadily increasing NCI over time. Whereas eTCR+/ rTCR± (purple) and eTCR-/

703 rTCR+ (green) groups show an initially increased NCI, followed by a marked decline.

704 Normalised to time point prior to effector T cell addition. **(ii)** Summary data of AUC.

705 Increased AUC values were observed at the lower E:T ratios, with eTCR-/ rTCR+ consistently

706 presenting with the lowest AUC values. Error bars ± 1 SEM. IFNγ: Interferon-γ, IL-2:

707 interleukin-2, CCL4: C-C motif chemokine ligand 4.

708

709 **Figure 4: Effector T cell cytokine responsiveness and target cell killing in a 3D microfluidics**

710 **device. A)** Flow cytometry based phenotyping of effector T cells used in 3D killing assay post

711 cryopreservation (gated on CD45+). **B)** Histogram depicting cytokine responsiveness of

712 effector T cells isolated from either outside the collagen gel (grey), or inside the collagen gel

713 (blue) after 24 hours (cells pooled from 3 replicate devices, gated on rTCR+CD8+;

714 unmodified cells gated on rTCR-CD8+). **C)** Normalised killing of target PreS1-GFP-HepG2 cells

715 in response to effector T cells groups presented as violin plot with median (solid black line),

716 and 25th/ 75th quartiles (dotted black lines). PreS1-GFP-HepG2 alone (orange) and 20%

717 DMSO (red) were used as negative and positive controls respectively. Increased cytotoxicity

718 was observed with eTCR-/rTCR+ (purple) effectors, compared to PreS1-GFP-HepG2 alone (*p*

719 < 0.0001), eTCR+/ rTCR- (green, *p* < 0.002), and eTCR+/ rTCR± (blue, *p* = 0.0001). Each point

720 represents a section of a 3D microfluidics device from n=3 technical replicates (3 sections

721 analysed per device). One way ANOVA with Tukey's multiple comparison test. **D)**

722 Visualisation of a region within the collagen gel. Addition of 20% DMSO resulted in cell

723 death (red), while PreS1-GFP-HepG2 target cells alone resulted in high viability (green).

724 Addition of effector T cells (blue), resulted in different degrees of target cell killing between
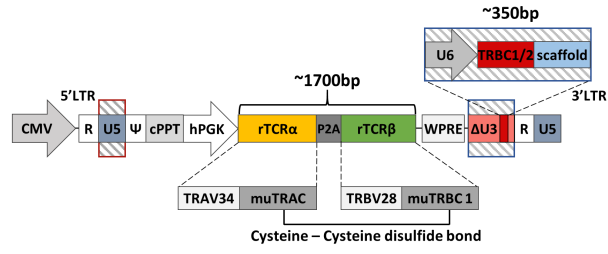
725 different effector groups (scale bar= 100µm).

726

727 **Figure 5: Molecular analysis of on-/off-target DNA editing, and fidelity of CDR3α and β**

728 **regions within rTCR mRNA transcripts. A)** Sanger sequencing of on-target editing at *TRBC*

729 *1/2* loci in eTCR-/rTCR+ cells. **i)** Representative EditR analysis with wild type sequence (top)

730 and four possible bases (side) shown at each position. Target G>A conversions (red box)

731 generate a premature stop codon (Trp>*). **ii)** Summary of EditR data for three donors at

732 cytosine positions 5 and 6 distal to the PAM, presented as C>T changes (black), non C>T

733 changes (grey) and no editing (white). Error bars ± 1 SEM **iii)** NGS sequencing analysis of on-

734 target editing of *TRBC 1/2* loci, quantification and characterisation of indels after BE3 editing

735 found only low levels of small (<10bp, black) or large indels (10-100bp, grey) with the

736 majority of reads presenting with no indels (white). Error bars ± 1 SEM. **B)** Box plots showing

737 off-target editing detected by NGS analysis at the top 6 *in silico* predicted off-target sites for

738 the TRBC 1/2 sgRNA, with comparison of unedited eTCR+/rTCR- and edited eTCR-/rTCR+

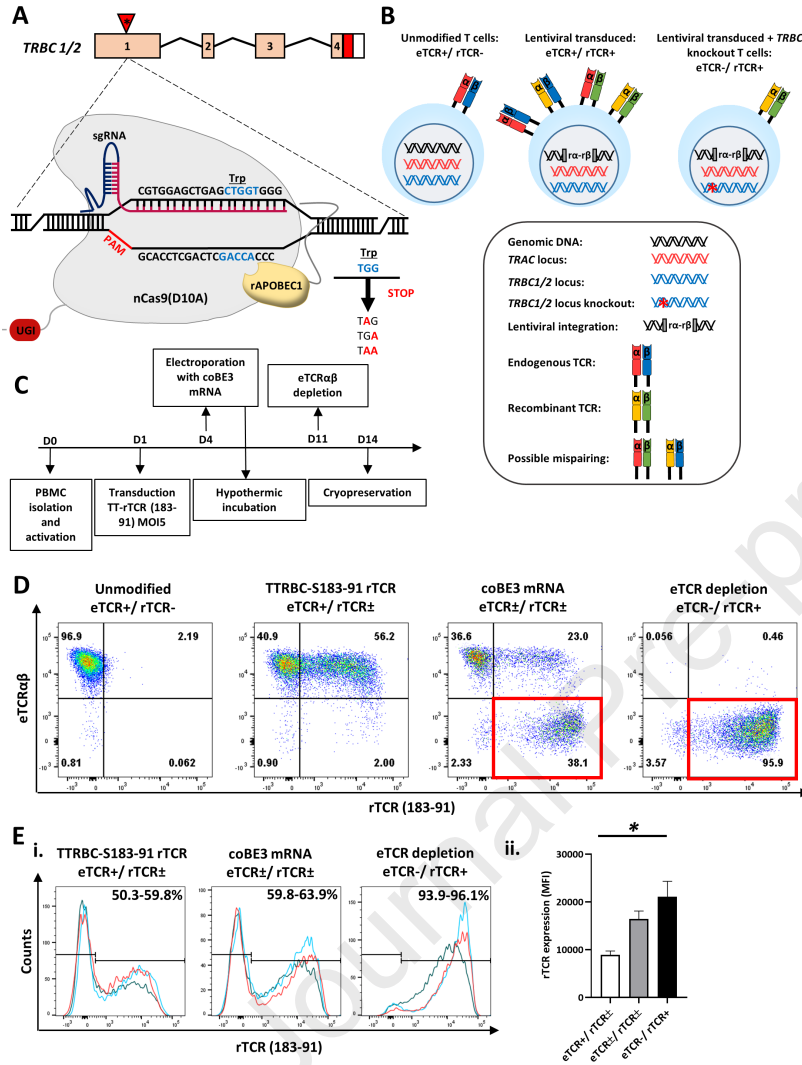739 groups (n=3). Larger dots represent outliers, in all cases ≤1.3% conversion. Two-tailed

740   independent t-test between unmodified (eTCR+/rTCR-), and edited (eTCR-/rTCR+) samples

741   shown for donor 1 *p* > 0.5, donor 2 *p* = 0.001, and donor 3 *p* > 0.1). **C)** Serial examination of

742   RNA from rTCR HBs183-91 for 8 days post coBE3 mRNA delivery (days 5-12 post activation)

743   found no evidence of promiscuous deamination, with fidelity of CDR3α and CDR3β regions

744   maintained. Amplicon positions are marked above for C residues and schematic highlights

745   hypervariable CDR3α and CDR3β regions that confer HLA-peptide specificity. CDR3 regions

746   were mapped as a Heatmap in R using the *gplots* library for C>T conversion rates at the

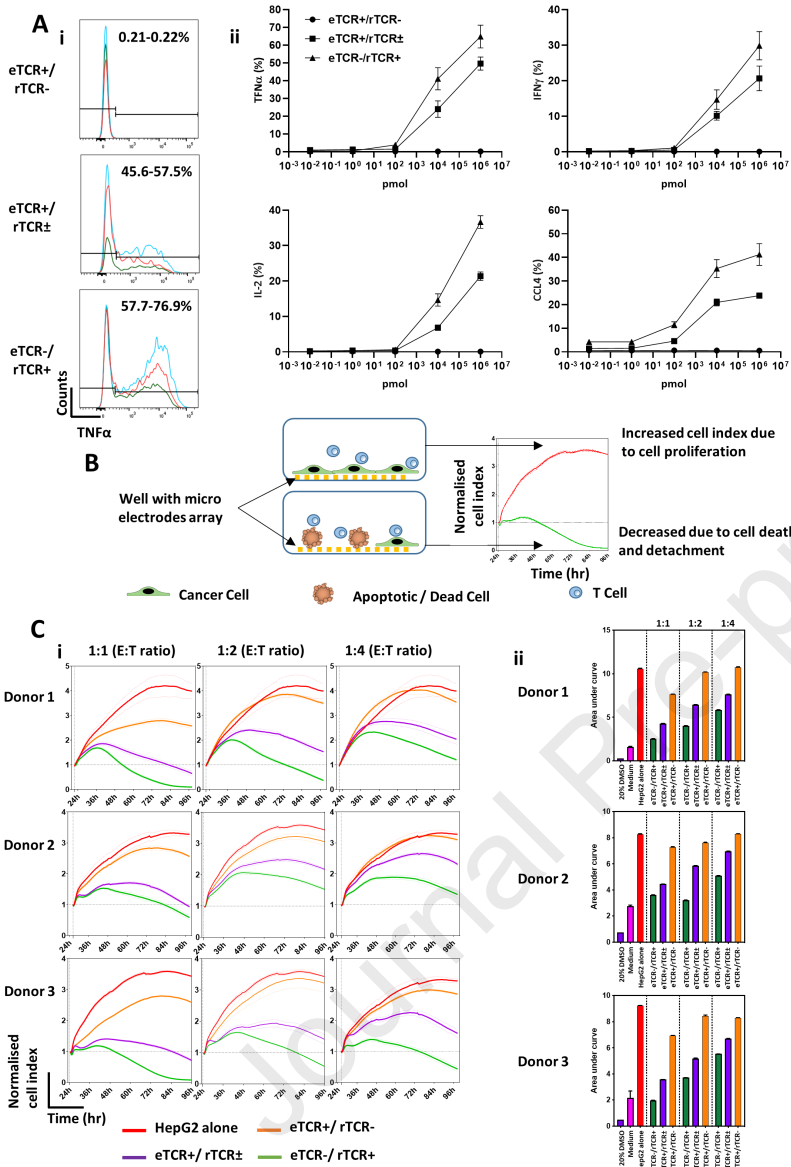747   marked sites (TCR Clone software: TCRmodel [66]).

The authors deploy cytosine deamination mediated base editing to genetically disrupt endogenous T cell receptors (eTCR), thereby reduce competition with recombinant TCRs (rTCR) and allowing enrichment of engineered T cells for immunotherapy against Hepatitis B driven hepatocellular carcinoma.
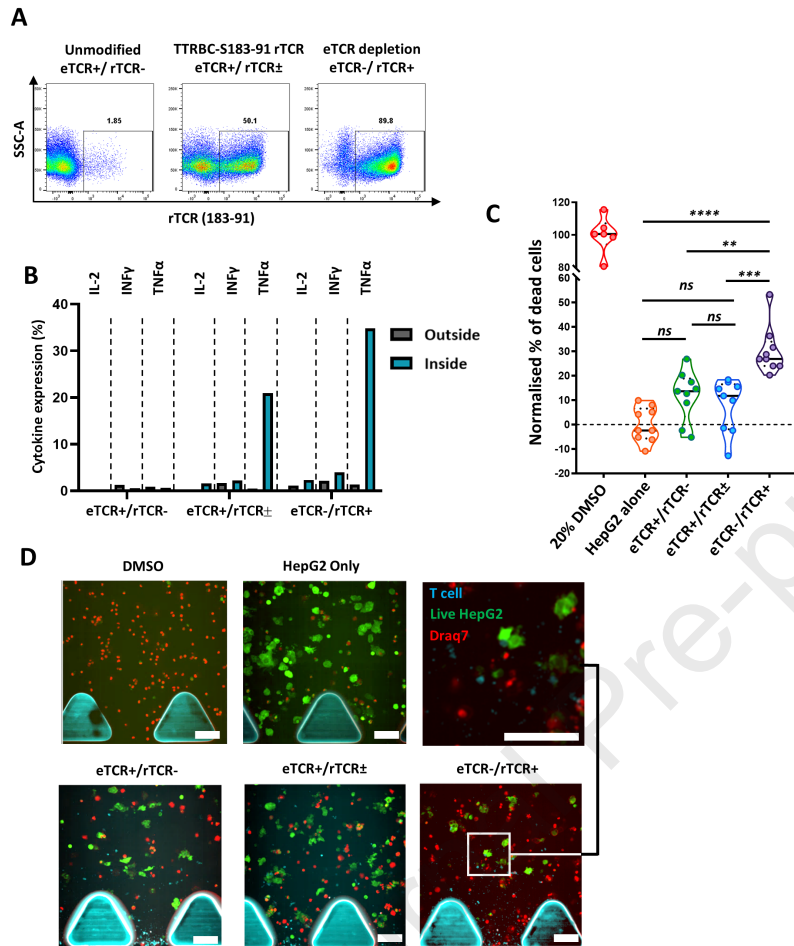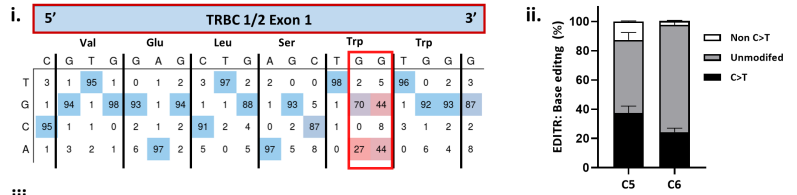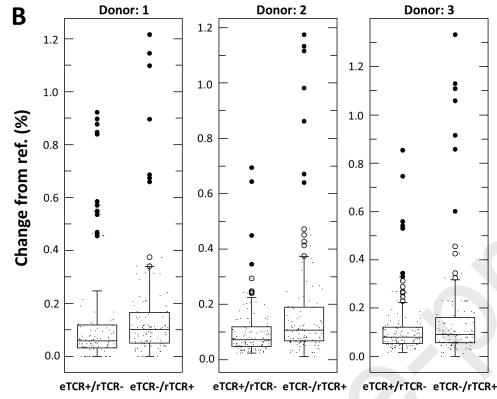
A

i

eTCR+/ rTCR- 0.21-0.22%

eTCR+/ rTCR± 45.6-57.5%

eTCR-/ rTCR+ 57.7-76.9%

Counts

TNFα

ii

- ● eTCR+/rTCR-
- ■ eTCR+/rTCR±
- ▲ eTCR-/rTCR+

TNFα (%)   pmol

IFNγ (%)   pmol

IL-2 (%)   pmol

CCL4 (%)   pmol

B

Well with micro electrodes array

Increased cell index due to cell proliferation

Decreased due to cell death and detachment

Normalised cell index

Time (hr)

Cancer Cell   Apoptotic / Dead Cell   T Cell

C

i

1:1 (E:T ratio)   1:2 (E:T ratio)   1:4 (E:T ratio)

Donor 1

Donor 2

Donor 3

Normalised cell index

Time (hr)

HepG2 alone   eTCR+/ rTCR-
eTCR+/ rTCR±   eTCR-/ rTCR+

ii

1:1   1:2   1:4

Donor 1

Area under curve

Donor 2

Area under curve

Donor 3

Area under curve

A

i.

ii.

iii.

B

Donor: 1   Donor: 2   Donor: 3

C

Colour Key: